HHS Public Access

Author manuscript

Nat Methods. Author manuscript; available in PMC 2014 June 01.

Published in final edited form as:

Nat Methods. 2013 December ; 10(12): 1203–1205. doi:10.1038/nmeth.2682.

Exclusive formation of monovalent quantum dot imaging probes by steric exclusion

Justin Farlow[1,2,3], **Daeha Seo**[4,5,6], **Kyle E. Broaders**[1], **Marcus Taylor**[7], **Zev J. Gartner**[1,2,3], and **Young-wook Jun**[4]

[1]Department of Pharmaceutical Chemistry, University of California, San Francisco, CA 94158, USA.

[2]Tetrad Graduate Program, University of California, San Francisco, CA 94158, USA.

[3]UCSF Center for Systems and Synthetic Biology, University of California, San Francisco, CA 94158.

[4]Department of Otolaryngology, University of California, San Francisco, CA 94115, USA.

[5]Department of Chemistry, University of California, Berkeley, CA 94720, USA.

[6]Materials Science Division, Lawrence Berkeley National Laboratory.

[7]Department of Cellular and Molecular Pharmacology, University of California, San Francisco, CA 94158, USA.

Abstract

Precise control over interfacial chemistry between nanoparticles and other materials remains a significant challenge limiting the broad application of nanotechnology in biology. To address this challenge, we use “Steric Exclusion” to completely convert commercial quantum dots (QDs) into monovalent imaging probes by wrapping the QD with a functionalized oligonucleotide. We demonstrate the utility of these QDs as modular and non-perturbing imaging probes by tracking individual Notch receptors on live cells.

Common strategies for chemically linking materials to nanoparticles generate products with valencies that follow a Poisson distribution due to the presence of multiple reactive sites at the particle surface[1]. For example, titration of QDs with increasing concentrations of a trithiolated DNA (ttDNA, **Fig. 1a**) generates an underdispersed Poissonion distribution of product valencies[2], where the desired monovalent QDs are always obtained alongside

Correspondence should be addressed to Z.J.G. (zev.gartner@ucsf.edu) or Y.J. (yjun@ohns.ucsf.edu)..

AUTHOR CONTRIBUTIONS

Z.J.G., J.F. and Y.J. conceived the study; J.F., Z.J.G. and Y.J. designed experiments; J.F., D.S., K.E.B., M.T., Z.J.G., and Y.J. performed experiments; J.F. and D.S. analyzed and interpreted the data; and J.F., Z.J.G., and Y.J. wrote the manuscript. All authors discussed and commented on the manuscript.

COMPETING FINANCIAL INTERESTS

The authors declare no competing financial interests.

Supplementary information is available in the online version of the paper

unconjugated and multivalent QD byproducts (**Fig. 1b** and **Supplementary Fig. 1**). Multivalent nanoparticles present in these mixtures complicate their use for biological imaging because of their potential for perturbing their target's function by oligomerization, leading to receptor activation, internalization, or redistribution on the cell surface[3-5]. These confounding properties of multivalent nanoparticles have motivated the development of methods for purifying monovalent QDs from more complex mixtures[5-9]. However, the low synthetic yield of these strategies, along with the multiple steps necessary to isolate pure monovalent QDs, have slowed their broad application in the biomedical sciences. More recent efforts have aimed to synthesize QDs of controlled valency without the need for purification[10,11]. These methods remain technically challenging for the typical researcher, generate products with low overall yield, or lack the necessary modularity to be broadly useful.

By nature of their large size, macromolecules or nanoparticles conjugated to QDs limit the maximum valency of products by sterically excluding a large fraction of the QD surface from additional reactions[10,12,13]. We also envisioned using this concept to synthesize monovalent QDs, but in quantitative yield, by using a polymer having only a modest per-monomer affinity for the nanoparticle surface to wrap the QD in a single synthetic step, irreversibly forming a monovalent product and simultaneously preventing the binding of a second polymer molecule by “Steric Exclusion” (**Fig. 1a**(bottom)). Ideally, this approach would produce monovalent QDs that retain their excellent photophysical properties, not add significantly to their size, work efficiently under homogeneous reaction conditions, form a stable colloidal product, use commercially available reagents as starting materials, and allow for modular conjugation to a variety of targeting molecules.

To implement this Steric Exclusion strategy, we used phosphorothioate DNA (ptDNA) as a polymer due to 1) the demonstrated affinity of phosphorothioates for semiconductor surfaces[10,14], 2) the ease of synthesizing ptDNA of precisely defined sequence and length, and 3) its availability to any researcher from most oligonucleotide synthesis companies. After transfer of commercial CdSe:ZnS QDs from the organic to the aqueous phase, we treated the QDs with ptDNA of various sequences and lengths. DNA-functionalization produced QDs with an ionic character that were easily distinguishable from unfunctionalized QDs by agarose gel electrophoresis[8,15]. We titrated 605 nm emitting QDs (605-QDs) with increasing concentrations of an oligonucleotide comprising a 50 adenosine ptDNA domain (A^{S}_{50}) and a 20 nucleotide ssDNA targeting tail (Fig. 1c, Supplementary Note 1, Supplementary Figs. 1 and 2). Agarose gel electrophoresis revealed a single band with increased mobility relative to starting materials indicating production of a single species (**Fig. 1b**). At stoichiometric or higher ratios of ptDNA and QD, no sign of unfunctionalized or multiply functionalized products were observed, consistent with the quantitative formation of a monovalent product (mQDs) (**Fig. 1d, Supplementary Figs. 1 and 3**). The strategy was also effective for generating mQDs with different size, shapes, and hence different emission spectra (**Fig. 1d**). QD-DNA conjugation was most efficient with oligonucleotides having a phosphorothioate backbone and adenosine bases (**Supplementary Fig. 4**).

The ptDNA-wrapped mQDs had excellent colloidal and photophysical properties in physiologically relevant buffers such as phosphate buffered salines (PBS) and culture media when passivated with commercially available polyethyleneglycol (PEG) ligands (**Supplementary Note 2, Supplementary Figs. 5-10**). The hydrodynamic diameter of 605-mQDs was narrowly distributed around 12 nm as measured by dynamic light scattering (DLS) – only 2 nm greater than bare particles (**Fig. 1e**).

We further investigated whether mQDs could be modularly and efficiently targeted to protein or lipid tags used frequently for live cell imaging. Targeting functionality was introduced by 3'-modification of the ptDNA or by hybridization of mQDs with complementary DNA bearing a 5'-modifcation. We used these strategies to conjugate mQDs with biotin, benzylguanine (BG), benzylcytosine (BC), and lipids, thereby targeting them to streptavidin, SNAP, CLIP, and cell membranes, respectively (**Fig. 1f, Supplementary Fig. 11-13**).

To provide more direct evidence for monovalency, we hybridized mQDs to gold nanocrystals bearing a single complementary sequence of ssDNA. We observed the formation of a single higher molecular weight band by gel electrophoresis, consistent with the exclusive formation of heterodimers (**Supplementary Fig. 14, Supplementary Note 3**). Analysis of this band by transmission electron microscopy (TEM) revealed nearly exclusive formation of mQD-Au heterodimers (n = 545, **Fig. 2a,b**). We rarely observed higher order structures, such as trimers (2%) and tetramers (<0.2%) by TEM (**Supplementary Fig. 15)**. In contrast, a reaction of multivalent Streptavidin QDots with similar DNA-linked monovalent gold nanocrystals conjugated to biotin resulted in multivalent products such as trimers and tetramers along with QD-Au heterodimers (Fig. 3a,b; Supplementary Fig. 14, Supplementary Note 4).

Previous studies reported that multivalent QDs generate imaging artifacts by triggering receptor clustering and endocytosis[3-5]. QD-mediated receptor clustering can also perturb the receptors' diffusion. To investigate whether mQDs crosslink protein targets, we prepared supported lipid bilayers (SLBs) incorporating His-tagged SNAP protein via a small fraction of NTA-linked lipid (**Fig. 2c**). We imaged the diffusion of the membrane-bound SNAP using a small organic dye, commercially available Streptavidin QDots, or mQDs (**Supplementary Video 1, Supplementary Note 4**) and analyzed several hundred single molecule trajectories for each probe. The diffusion coefficient measured using the Streptavidin QDots was significantly lower than using the dye (p = 0.001). The diffusion further slowed at higher SNAP protein density (**Fig. 2c, Supplementary Fig. 16**.), consistent with the notion that multivalent Streptavidin QDots crosslink the target (**Fig. 2c; Supplementary Figs. 17 and 18**). In contrast, we observed a nearly identical distribution of diffusion coefficients for mQDs and the dye, independent of protein density (**Fig. 2c**). These data indicate that mQDs behave as *bona fide* and non-perturbing single molecule imaging agents in model cell membranes.

We next applied these small, modular, and monovalent QDs to track individual Notch receptors on live cells. Notch activation plays a central role in cell fate decisions during development, normal tissue maintenance and cancer[16]. Despite its importance in these

biological processes, little is known about the dynamics of Notch receptors at the cell surface. We aimed to measure the diffusion coefficient of single notch receptors in order to reveal whether diffusion of Notch receptors is dominated by interactions with the viscous lipid bilayer or by surrounding proteins and glycans on the cell surface and cortex. To track Notch, we inserted a SNAP tag onto the N-terminus of a previously reported human Notch1 construct and expressed the resulting protein (SNAP-Notch) in U2OS cells (**Supplementary Fig. 19**)[17]. The BG-mQDs labeled the cells expressing SNAP-Notch (red fluorescent cells) with high specificity. Negligible binding was observed to cells expressing a control GFP-Notch construct lacking the SNAP tag (green fluorescent cells; **Fig. 3a, Supplementary Fig. 20 and 21**).

To confirm that the mQDs did not alter the mobility of Notch on live cells, we tracked SNAP-Notch labeled with mQDs and compared their average diffusion coefficients to receptors labeled with BG-Alexafluor-647 on the same cell (**Fig. 3b, c** and **Supplementary Video 2**). Analysis of mean-square-displacement (MSD) versus time revealed mean diffusion coefficients (*D*) of 0.081 and 0.076 $\mu m^2/s$ ($p = 0.7255$) for Notch imaged with Alexa-647 and mQDs, respectively. The measured diffusion constant of Notch deviates from other freely diffusing single pass transmembrane proteins tracked by fluorescence microscopy (0.17-0.5 $\mu m^2/s$)[18,19]. The observed differences are not a consequence of cell type or imaging conditions, as a minimal protein based on the type I transmembrane domain from CD86 in U2OS cells also yielded an apparent diffusion coefficient (0.29 $\mu m^2/s$) several fold higher than Notch (**Fig. 3c**). In contrast, measured diffusion coefficients for Notch are consistent with reported values of single pass transmembrane proteins known to interact with components of the cell surface or cell cortex[18-20]. Although the physical source of the slow diffusion remains to be determined, our measurements suggest that the diffusion of Notch is dominated by interactions with proteins or glycans, rather than the viscous lipid bilayer.

In conclusion, we report a potentially general method for preparing nanoparticles of fixed targeting valency using the principle of Steric Exclusion. The method is likely applicable to other nanoparticle materials using either modified nucleic acids or other polymers of low dispersity and controlled chemical functionality. We apply this simple method to prepare ptDNA-wrapped mQDs in quantitative yield and from commercially available starting materials. mQDs prepared by Steric Exclusion retain their small size and excellent photophysical properties, and incorporate a single, modular targeting functionality. As a consequence of their monovalency, they do not perturb the diffusion of biomolecules in model membranes or live cells. The facile preparation of these small, bright, monovalent, and modular imaging probes make them accessible to any researcher with basic molecular biology tools and reagents. Therefore mQDs should find broad utility in biophysical and cell biological studies requiring single molecule imaging, either *in vitro* or in live cells.

ONLINE METHODS

Reagents

Organic quantum dots (Purchased from Invitrogen, Sigma-Aldrich, or Ocean Nanotech Inc.; **Supplementary Fig. 22**), chloroform (ACROS, 99.8%), tetrabutylammonium bromide

(TBAB, Sigma-Aldrich, 98.0%), 2,5,8,11,14,17,20-heptaoxadocosane-22-thiol (mPEG thiol, Polypure, MW 356.5, 95%), HS-$(CH_2)_{11}$-$(OCH_2CH_2)_6$-OCH_2CO_2H ($HSC_{11}EG_6CO_2H$, ProChimia), streptavidin (Thermo Scientific), gold(III) chloride trihydrate (or hydrogen tetrachloroaurate, $HAuCl_4 \cdot 3H_2O$, Aldrich, >99.9%,), bis(p-sulfonatophynyl) phenylphosphine dehydrate dipotassium salt (BSPP, Aldrich, 97%), boric acid (Sigma-Aldrich, 99.5%), sodium hydroxide (ACROS, 99.0 %), sodium chloride (NaCl, Sigma, 98%), Agarose LE (U.S. Biotech Sources), Ficoll (Fisher BioReagents), Rhodamine 6G (R6G), ethanol (sigma-aldrich). All reagents were used without further purification except QDs stabilized with amine ligands. These QDs were ligand-exchanged by reacting them with trioctylphosphine oxide (1g, Sigma-Aldrich, 90%) in $CHCl_3$ (10 ml) under inert atmosphere for 30 min. Gold nanoparticles (4 nm) were synthesized according to the literature method[21], and then conjugated with single stranded DNA (5'-trithiol-$(GTCA)_5$). Singly modified gold-DNA nanoparticles were purified by a literature method[6].

Instruments and Characterization

The Dynamic Light Scattering (DLS) measurements were performed with a Malvern Zetasizer Nano zs90. Transmission Electron Microscope (TEM) images were taken using a Tecnai G220 S-TWIN at an acceleration voltage of 200 kV. Flow cytometry was performed on a BD FACSCaliber & FACSAria II. TIRF (total internal reflected fluorescence) Microscopy was performed on a Nikon Eclipse TI. Confocal microscopy was carried out on a Zeiss Axio Observer Z1. Absorption spectra of QDs were obtained with either Shimadzu UV-1650 PC or HP8453. The quantum yield of QDs (Φ_x) was measured by a FP-6500 (Jasco) spectrofluorometer with 490-nm excitation following a literature method[22].

$$\Phi_x = \Phi_{st} \left(F_x f_{st}(\lambda_{ex}) \, n_x^2 \right) / \left(F_{st} f_x(\lambda_{ex}) \, n_{st}^2 \right)$$

where, Φ_{st} is fluorescence quantum yield of a dye (R6G) using the reported value of 0.95 in ethanol, and used as a reference, F is the integrated emission spectrum, $f(\lambda_{ex})$ is the absorption factor given by $f_x(\lambda_{ex}) = 1\text{-}10^{-A(\lambda ex)}$ ($A(\lambda_{ex})$ is a absorbance at the excitation wavelength), and n is the refractive index of media (1.313 for water and 1.360 for ethanol).

Synthesis of phosphorothioate oligonucleotides

Oligonucleotides were synthesized using an Expedite DNA synthesizer by standard phosphoramidite chemistry and deprotected for 15 minutes at 65 °C using AMA (ammonium hydroxide:methylamine 50:50). Phosphoramidites and synthesis reagents were purchased from Glen Research and AZCO Biotechnology. Phosphorothioate containing oligonucleotides were synthesized by replacing the standard oxidizing solution with 1 % DDTT (3-((Dimethylamino-methylidene)amino)-3H-1,2,4-dithiazole-3-thione, Glen Research) dissolved in 60:40 pyridine:acetonitrile, and were prepared DMT(dimethoxytrityl)-ON. All oligonucleotides were purified using an Agilent 1200 HPLC equipped with Zorbax XDB-C8 semi-preparative column running an acetonitrile/0.1M TEAA (triethylamine acetate) mobile phase. Purified phosphorothioate oligonucleotides retained the 5'-DMT protecting group and were used without further modification after lyophilization.

Phase transfer of organic QDs into aqueous phase

To organic QDs (3.0 mL in chloroform), TBAB (2.0 mL, 0.3 M in chloroform) and mPEG thiol (180 μL) were added. After 30 min, aqueous NaOH (4.0 mL, 0.2 M) was added to this mixture. The mixture was briefly vortexed and centrifuged at 1,000 g for 30 sec to completely separate the phases. The aqueous layer was recovered and the collected QDs were concentrated using a centrifugal (30 kDa, Amicon) device, and then purified by NAP desalting column (GE Healthcare) with Tris 10 mM containing 30 mM NaCl (pH 8) as an eluent. QD concentration was determined by absorbance at 350 nm (extinction coefficients of QD 545, 585 and 605 at 350 nm are 1,590,000, 3,500,000, and 4,400,000 $M^{-1}cm^{-1}$, respectively).

Preparation of ptDNA-mQDs

To confirm the exact 1:1 stoichiometry of DNA vs. QDs, we first added 0.5 equivalents of ptDNA (100 nM, 0.5 mL) to QDs (100 nM, 1 mL), dropwise under vigorous stirring. We found that dropwise addition is critical for exclusive formation of mQDs (**Supplementary Fig. 23**). After 9 h reaction, DNA conjugation of QDs was confirmed by electrophoresis using Mini-Sub Cell GT cell (Biorad) with 0.8 % Superpure agarose (U.S. Biotech Sources) in sodium borate buffer at 8 V/cm for 15 min. The conjugation yield was determined by relative fluorescence intensity between two bands on an agarose gel corresponding bare and monovalent QDs. We then added an appropriate amount of ptDNA solution (based on the above calculation) and the mixture was further reacted for 9 h. For further reactions with biomolecules or cell surface receptors, the surface ligands were exchanged with $HSC_{11}H_{23}(OCH_2CH_2)_6OCH_2CO_2H$ ($x10^4$ equiv. of QDs) for 10 min. The resulting solution was concentrated to 0.2 ml and then desalted with a NAP-10 column prior to use. No noticeable aggregation of QDs after DNA conjugation was observed (**Supplementary Fig. 24**).

Modular conjugation of mQDs

a. Monovalent QD-X (X = biotin, BG, or BC)—Biofunctional moieties can be easily added to mQDs either by directly incorporating a desired functional group (ex. biotin) at the 3’-end of DNA to be conjugated or by incorporation into the complementary strand (ex. BG-DNA, BC-DNA). Hybridization reactions were performed as follows: to a solution containing mQDs bearing $(ACTG)_5$ tail (500 μL of a 50 nM solution in 10 mM Tris, 100mM NaCl) were added to 10 equiv. of X-$(CAGT)_5$ (25 μM, 10 μL). After 6 h, excess complementary DNAs were removed by a centrifugal filter device (MWCO 30 kDa, Amicon). The functionality of the monovalent QD-Xs was confirmed by incubating 10 equivalents of target biomolecules (streptavidin, SNAP, or CLIP) at 4 °C for 5 h. Quantitative reaction was confirmed by agarose gel electrophoresis.

b. QD-Au hybridization—mQDs bearing a $(CAGT)_5$ tail were treated with 10 equivalents of Au nanoparticles bearing a single complementary sequence of ssDNA in Tris buffer (10 mM Tris 200 mM NaCl, pH 8). Separately, Streptavidin QDots (Life Technology, QD605) were treated with 10 equivalents of Au nanoparticles bearing a single biotinylated ssDNA under same reaction conditions. Monovalent Au nanoparticles were synthesized via

literature methods and surface modified with either HS-$C_3H_7(OCH_2CH_2)_6OCH_3$ (mPEG-SH) or HS-$C_3H_7(OCH_2CH_2)_6OCH_2$-COOH (COOH-PEG-SH). After overnight reaction, the coupling efficiency was determined by an agarose gel electrophoresis using Mini-Sub Cell GT Cell (Biorad) with 2 % Superpure agarose (U.S. Biotech Sources) in sodium borate buffer at 10 V/cm for 20 min. Bands exhibiting both Au color and QD fluorescence were extracted via electrodialysis and then dropcasted onto a carbon-coated copper TEM grid for imaging. Statistical analysis of QD valency was performed by counting number of Au nanocrystals per QD (**Supplementary Fig. 15**)

Imaging SNAP-protein diffusion in supported lipid bilayers

Small, unilamellar vesicles (SUVs) containing 97.5 % 1,2-dioleoyl-3-sn-phosphatidylethanolamine (DOPE), 2 % 1,2-dioleoyl-*sn*-glycero-3-[(N-(5-amino-1-carboxypentyl)-iminodiacetic acid)succinyl]Nickel (DGS-Ni-NTA) and 0.5 % 1,2-dioleoyl-sn-glycero-3-phosphoethanolamine-N-[methoxy(polyethylene glycol)-5000] (ammonium salt) were deposited onto well-cleaned glass surfaces. Surfaces were washed with phosphate buffered saline (PBS) containing 1 % bovine serum albumin (BSA), then incubated with DNA-linked SNAP protein; 5 μM 10x His-tagged SNAP dyed with NHS-Atto488 incubated with 5 μM BG-DNA (BG-$(CAGT)_5$) for 30 min at room temperature. Surfaces were further washed and then incubated with either mQDs bearing $(CT)_{10}(ACTG)_5$ or, biotin-DNA (biotin-$(CT)_{10}(ACTG)_5$) followed by commercial Streptavidin 605 QDots. Surfaces were imaged at 32 °C in (TIRF) mode with a 100x objective lens using either a 405 nm or 491 nm laser at 20 Hz on a Hamamatsu ImagEM electron multiplying charge coupled device (EM-CCD).

Cloning and cell lines

SNAP-Notch was constructed by cloning the SNAP-tag (NEB) onto the N-terminus (but behind both the signal sequence and flag tag) of a flag-tagged Notch-Gal4 construct (a kind gift from Stephen Blacklow, Harvard University). U2OS-Notch-GFP along with a U2OS FLP-In line containing the Tet repressor were also kind gifts from Steven Blacklow. Snap-Notch was flipped into the U2OS cell line per Invitrogen's protocol; briefly, cells were cotransfected with FLP-recombinase, pOG44 and the above SNAP-Notch construct using Lipofectamine 2000 followed by selection with 400 μg/ml Hygromycin for 10 days. Cells were cultured in McCoy's 5A media with 10 % FBS and passaged every 3-4 days. Jurkat cells were cultured in RPMI containing HEPES and 10 % FBS. All cells were maintained at 37 °C and in 5 % CO_2 in a humidified incubator.

Live cell labeling and imaging

Unless otherwise noted, cells were incubated with 1 μM BG-DNA for 30 minutes at 37 °C, washed three times with PBS containing 1 % BSA, and then incubated with 200 pM mQDs for 5 minutes at room temperature before a final wash with 1 % BSA. In dye-comparison experiments, cells were incubated simultaneously with 1 μM BG-DNA and 0.2 μM BG-AF647 (Surface-SNAP-647, NEB). For single particle tracking, mQDs were incubated in PBS containing 1 % BSA for 30 min at room temperature prior to being added to cells at a concentration of 0.2 nM. For high-density labeling mQDs were incubated in 5 % Alkali-

soluble Casein (EMD Millipore) prior to being added to cells at a concentration of 5 nM. Live cells were imaged on a Ti Nikon Eclipse inverted microscope (use courtesy of the UCSF Cardiovascular Research Institute) at 37 °C with 5 % CO_2. Two 30-second movies were acquired in sequence at 20 Hz; first with dye, and then with mQDs. QDs were imaged using a 488 nm laser from an Agilent Technologies MLC 400B.

Flow Cytometry

Jurkat cells were labeled with DNA according to published procedure[23]. Briefly, cells were incubated for 5 minutes at room temperature with 5.5 μM of a Lipid-DNA sequence identical or complimentary to that on the QDs. Cells were washed 3x with PBS containing 1 % BSA and then incubated with 5 nM mQDs for 5 minutes at room temperature before additional washing with PBS/BSA. Cells were then analyzed using a BD FACS-Aria flow cytometer using the 405 nm laser coupled with a 610/20 filterset.

High-density labeling of cells with dyes & QDs

Both Snap-Notch & Notch-GFP expressing cells were cocultured in 8-well chamber slides for 48 h in the presence of 1 μg/ml doxycycline. For high-density images, cells were fixed using 5 % formaldehyde and then immediately imaged via confocal microscopy. QDs were excited using a 405 nm laser. Nuclei were stained with either DAPI when staining was done with AF647, or with DRAQ5 when stained with the QDs, as DAPI fluorescence bleeds into the QD channel.

Background binding measurements

For low-density (200 pM) signal/noise (S/N) measurements, images were obtained under single-particle tracking conditions on a TIRF microscope, but for 1 s rather than 0.05 s exposures. For high-density (5 nM) S/N measurements, images were obtained from fixed samples on a confocal microscope. QDs within comparable regions of interest on both ‘green’ and ‘non-green’ cells were counted using the ‘Localization Microscopy’ plugin in μManager. At least 120 1,089 μm^2 regions of interest across two labeling experiments and ten different fields were used to calculate S/N.

Supplementary Material

Refer to Web version on PubMed Central for supplementary material.

ACKNOWLEDGEMENTS

The authors thank B. van Lengerich, L. D. Hughes and P. Haggie for assistance with single particle tracking software. S. Blacklow (Harvard University) provided hNotch1 constructs. R. Vale (UCSF) provided feedback on the single molecule imaging analyses. A. P. Alivisatos (UC Berkeley) provided helpful discussion. J. Taunton and the CVRI Core provided TIRF microscopes. N. Sturman helped with localization microscopy plugin. B. Liang and K. Southard & M. Todhunter generated some preliminary data. J.F. was supported by the UCSF Center for Synthetic and Systems Biology (P50 GM081879). D.S. was supported by Human Frontier Science Program – Cross disciplinary postdoc research fellowship. Z.J.G. was supported by Kimmel Family Foundation. Y. J. was partly supported by 1R21EB015088-01 from the National Institute of Biomedical Imaging and Bioengineering and National Institutes of Health and the Bryan Hemming Fellowship.

References

1. Pons T, Medintz IL, Wang X, English DS, Mattoussi H. J. Am. Chem. Soc. 2006; 128:15324–15331. [PubMed: 17117885]
2. Shmueli G, Minka TP, Kadane JB, Borle S, Boatwright P. Journal of the Royal Statistical Society: Series C (Applied Statistics). 2005; 54:127–142.
3. Saxton MJ, Jacobson K. Annu. Rev. Biophys. Biomol. Struct. 1997; 26:373–399. [PubMed: 9241424]
4. Banerjee D, Liu AP, Voss NR, Schmid SL, Finn MG. ChemBioChem. 2010; 11:1273–1279. [PubMed: 20455239]
5. Howarth M, et al. Nat. Methods. 2008; 5:397–399. [PubMed: 18425138]
6. Zanchet D, Micheel CM, Parak WJ, Gerion D, Alivisatos AP. Nano Lett. 2001; 1:32–35.
7. Clarke S, et al. Nano Lett. 2010; 10:2147–2154. [PubMed: 20433164]
8. Carstairs HMJ, Lymperopoulos K, Kapanidis AN, Bath J, Turberfield AJ. ChemBioChem. 2009; 10:1781–1783. [PubMed: 19554595]
9. You C, et al. Angew. Chem. Int. Ed. Engl. 2010; 49:4108–4112. [PubMed: 20432494]
10. Tikhomirov G, et al. Nat. Nanotechnol. 2011; 6:485–490. [PubMed: 21743454]
11. You C, et al. ACS Chem. Biol. 2013; 8:320–326. [PubMed: 23186299]
12. Wilson R, Chen Y, Aveyard J. Chem. Commun. 2004:1156–1157.
13. Montenegro J-M, et al. Adv. Drug Deliv. Rev. 2013; 65:677–688. [PubMed: 23280372]
14. Jiang L, et al. Chemical Physics Letters. 2003; 380:29–33.
15. Claridge SA, Liang HW, Basu SR, Fréchet JMJ. Alivisatos, A. P. Nano Lett. 2008; 8:1202–1206. [PubMed: 18331002]
16. Bray SJ. Nat. Rev. Mol. Cell Biol. 2006; 7:678–689. [PubMed: 16921404]
17. Gordon WR, et al. Blood. 2009; 113:4381–4390. [PubMed: 19075186]
18. Douglass AD, Vale RD. Cell. 2005; 121:937–950. [PubMed: 15960980]
19. Triantafilou M, Morath S, Mackie A, Hartung T, Triantafilou K. J. Cell. Sci. 2004; 117:4007–4014. [PubMed: 15286178]
20. Cairo CW, et al. J. Biol. Chem. 2010; 285:11392–11401. [PubMed: 20164196]
21. Jana NR, Gearheart L, Murphy CJ. Langmuir. 2001; 17:6782–6786.
22. Grabolle M, et al. Analytical Chemistry. 2009; 81:6285–6294.
23. Selden NS, et al. J. Am. Chem. Soc. 2012; 134:765–768. [PubMed: 22176556]

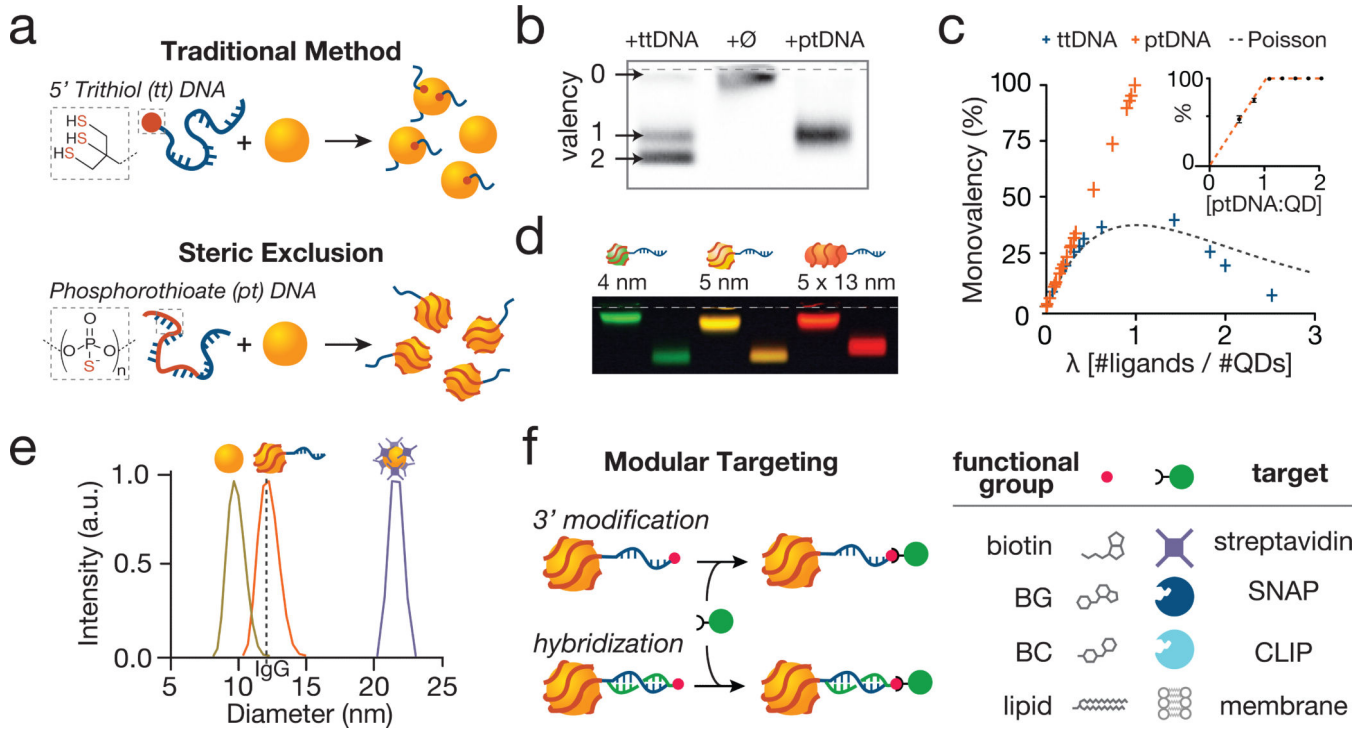

Figure 1. Exclusive synthesis of small, modular, and monovalent quantum dots (QDs) by the principle of Steric Exclusion

(**a**) Incubation of bare QDs with trithiol DNA (ttDNA) generates products with a distribution of valencies due to excess nanoparticle surface area. In contrast, phosphorothioate DNA (ptDNA) molecules of appropriate size wrap the nanoparticle, preventing the reaction of a second strand due to Steric Exclusion. (**b**) Agarose gel electrophoresis of reactions of ptDNA and ttDNA of identical length with bare nanoparticles optimized for yield of monovalent products. (**c**) Plot of lambda (average number of molecules bound per QD) versus percent monovalent products using ttDNA and ptDNA. Fitting the curve with a Poisson distribution indicates that the distribution of products generated by ttDNA is underdispersed relative to expected values for large lambda. The same curve for ptDNA is not defined for values of lambda greater than one. (inset) Plot of reaction stoichiometry (ptDNA:QD) versus percent monovalent products. (**d**) Steric Exclusion using 50 adenosine ptDNA sequences efficiently generated monovalent nanoparticles of distinct sizes, shapes, and hence spectral properties. (**e**) Dynamic light scattering analysis reveals that ptDNA-wrapped mQDs are 12 nm in diameter, similar in size to an IgG (dotted line) and about half the size of conventional Streptavidin QDots (22 nm). (**f**) DNA-wrapped mQDs can be selectively targeted by 3'-modification of the oligonucleotide. Alternatively, complementary strands bearing a 5' targeting modification such as benzylguanine (BG), benzylcytosine (BC) or lipid allow modular targeting of mQDs to streptavidin, SNAP-, CLIP-tags, or cell surfaces.

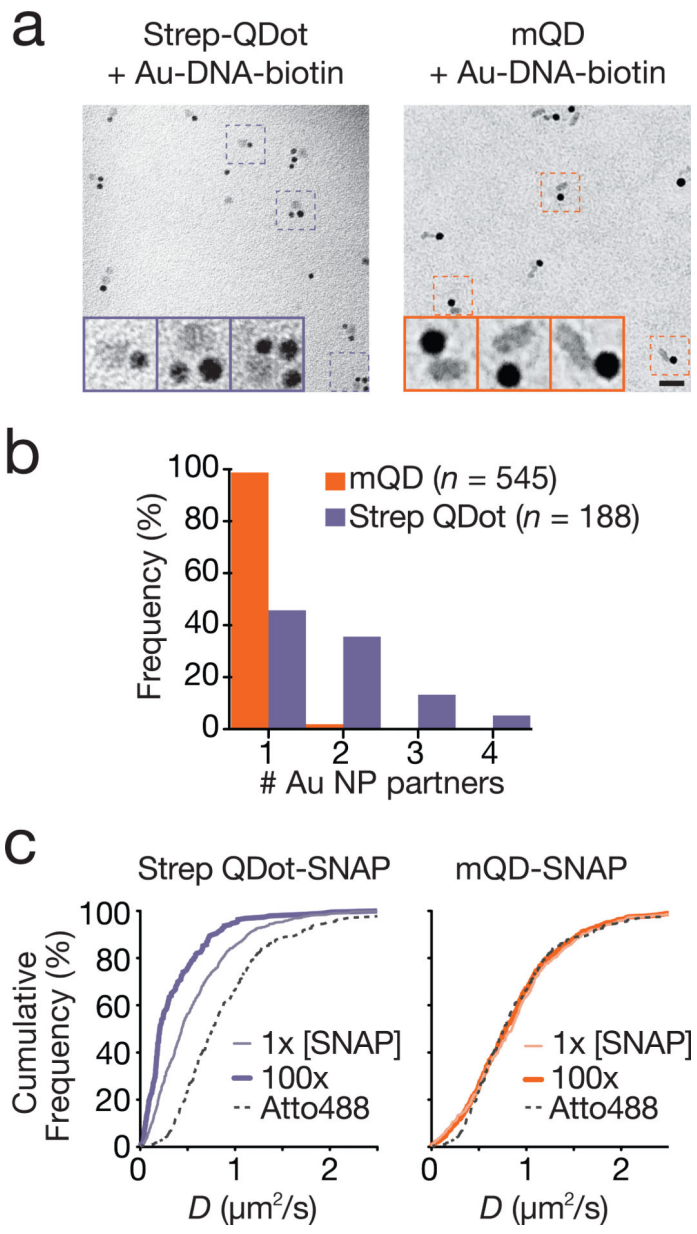

Figure 2. ptDNA-wrapped QDs are monovalent and do not oligomerize protein targets on supported lipid bilayers

(a) Representative TEM images of (left) commercial Streptavidin QDots incubated with gold nanoparticles bearing a biotinylated DNA sequence and (right) mQDs hybridized with gold nanoparticles bearing a complementary ssDNA sequence. (**b**) Statistical analyses of QD valencies from TEM images reveals the monovalent character of mQDs (Orange bars, *n*=545) compared with Streptavidin QDots (purple bars, *n*=188). (**c**) Distribution of diffusion constants of streptavidin-linked SNAP proteins on supported lipid bilayers (thin purple line, *n*=756, 0.56 μm^2/s mean) shows a decrease when the concentration of protein is increased 100 fold (thick purple line, *n*=189, 0.35 μm^2/s mean). Distribution of diffusion constants of mQD-linked SNAP proteins (thin orange line, *n*=490, 0.89 μm^2/s mean) is not altered when protein concentration is increased 100-fold (thick orange line *n*=790 0.86

μm^2/s mean). SNAP protein diffusion rates measured with mQDs are nearly identical to diffusion rates measure with small organic dyes such as Atto488 (dotted black line, *n*=245, 0.89 μm^2/s mean). Scale bar = 25 nm.

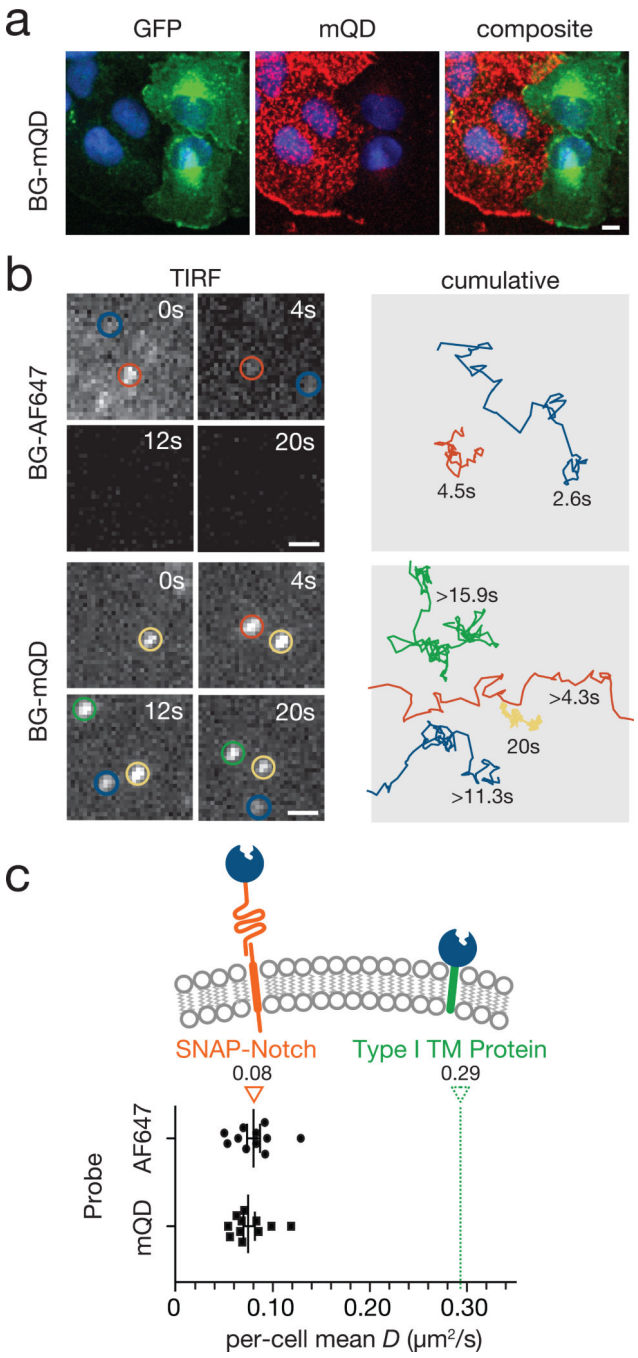

Figure 3. Diffusion dynamics of SNAP-Notch proteins on live cell surfaces

(**a**) Cocultures of U2OS cells expressing either SNAP-Notch or Notch-GFP incubated with 1 μM BG-AF647 or 1 μM BG-DNA and complementary mQDs. In both cases, specific labeling of SNAP-Notch proteins was clearly seen by confocal fluorescence microscopy. Scale bar = 10 μm. (**b**) Snapshots from the same region on the same cell showing trajectories of single SNAP-Notch proteins visualized by BG-AF647 and BG-mQD. Scale bar =1 μm. The complete trajectories are shown at the right panel. Some mQDs diffuse in and out of the field of view. (**c**) The mean diffusion constant of at least 15 SNAP-Notch proteins per cell

measured with both BG-mQDs or BG-Alexafluor dyes. No statistically significant difference in diffusion was found via t-Test ($p = 0.726$). The mean diffusion constant of a SNAP protein fused to an unrelated type I transmembrane domain from CD86 is shown as reference.

Table 1

DNA sequences used for conjugation with QDs

Conjugation experiments	Sequence of QD conjugated DNA	Total length of oligonucleotides	Sequence of complementary DNA
QD-ttDNA	5'- trithiol-$T_{50}m_1$ -3' m_1=AGT GAC AGC TGG ATC GTT AC	70 mer	-
QD-poly-A^S ptDNAs (X =A, T, or C)	5'-$A^S_{20}(m_1)_{2.5}$ -3'	70 mer	-
	5'-$A^S_{35}(m_1)_{1.75}$ -3'		
	5'- $A^S_{50}m_1$ -3'		
	5'- $A^S_{70}m_1$ -3'	90 mer	
QD-poly-X^S ptDNAs (X =A, T, or C)	5'- $A^S_{50}m_1$ -3' 5'- $T^S_{50}m_1$ -3' 5'- $c^S_{50}m_1$ -3'	70 mer	-
QD-Au	5'- $A^S_{50}(CAGT)_5$ -3'	70 mer	5'-Au nanoparticle-$(CT)_{10}(ACTG)_5$-3'
QD-streptavidin	5'- $A^S_{50}m_1$-biotin -3'	70 mer	-
QD-SNAP	5'-$A^S_{50}(ACTG)_5$ -3'	70 mer	5'-benzylguanine-$(CAGT)_5$-3'
QD-CLIP	5'- $A^S_{50}(ACTG)_5$ -3'	70 mer	5'-benzylcytocine-$(CAGT)_5$-3'
Notch imaging	5'- $A^S_{50}(CT)_{10}(ACTG)_5$ -3'	90 mer	